Life cycle assessment of building envelopes manufactured through different 3D printing technologies

Iacopo Bianchi [a], Stelladriana Volpe [b], Francesco Fiorito [b], Archimede Forcellese [a], Valentino Sangiorgio [c,*]

[a] *Department of Industrial Engineering and Mathematical Sciences (DIISM), Polytechnic University of Marche, Via Brecce Bianche 12, Ancona, 60131, Italy*
[b] *Department of Civil, Environmental, Land, Building Engineering and Chemistry (DICATECh), Polytechnic University of Bari, Via Edoardo Orabona, 4, Bari, 70125, Italy*
[c] *Department of Engineering and Geology (INGEO), D'Annunzio University of Chieti – Pescara, Viale Pindaro, 42, Pescara, 65127, Italy*

ABSTRACT

The advent of 3D printing technology in the construction field, as for many other industries, represents a technological upgrade. It introduces a paradigm shift in the way we approach construction and architecture, opening up new horizons and unprecedented possibilities. Indeed, due to its ability for infill optimization and reduction in material consumption, additive manufacturing (AM) can represent a sustainable solution for high-performance construction.

While there is a growing body of literature on 3D concrete printing (3DCP), several aspects related to sustainability remain unexplored. Systematic studies assessing the sustainability of various 3D printing technologies and techniques to achieve a building envelope are missing in related literature.

The present study fills a crucial gap in the literature by focusing on the environmental impacts and thermal properties of building envelopes achieved using three distinct emerging AM technologies and techniques. These technologies include large gantry cranes, small gantry cranes based 3D concrete printers, and Fused Deposition Modelling (FDM), applied in *monolithic construction*, *prefabrication*, and 3D-printed thin formwork for cast concrete components. The novelty of the proposed research is twofold. Firstly, it explores how different technologies and techniques can achieve target thermal performances for building envelopes through parametric modelling and thermal simulations. Secondly, it conducts a Life Cycle Assessment (LCA) analysis to identify the advantages of various 3D printing technologies and techniques in the context of building envelopes.

The results showed that the investigated 3D printing technologies have low energy consumption and can represent a sustainable alternative to traditional structures. The impacts of different technologies can vary significantly depending on the configuration and internal infill; this is mainly due to the quantity of concrete used, which can account for up to 95 % of the total impacts. Hence, the sustainability of envelopes can be improved using configurations with thinner wall thickness (i.e., obtained with prefabrication or FDM-based formwork technique).

By providing a better understanding of the sustainability aspects of these technologies, the study provides valuable insights for future developments in the field, guiding the construction industry towards more sustainable and innovative practices.

1. Introduction

The introduction of 3D printing in the field of construction brought about an unprecedented impact, introducing new and unexplored possibilities in the Architecture, Engineering, and Construction sector. In this context, the imperative for the construction industry to adopt 3D printing technologies of escalating magnitude becomes clear through the noticeable upsurge in investments both at the European and global levels (Volpe et al., 2022). Recent reports regarding companies' investments in 3D concrete printing (3DCP) indicate a remarkable trend of exponential growth for this technology (Grandviewresearch, 2023, Marketsandmarkets). Indeed, the utilization of 3D printing in the

domain of construction and civil engineering can be characterized as a disruptive technological advancement (Khan et al., 2020), as it fundamentally transforms the conventional constructive technique of the construction sector (Hossain et al., 2020). This transformation is attributed to the undeniable advantages it holds over traditional construction methodologies (Sati et al., 2021; Xiao et al., 2021). Indeed, Additive manufacturing (AM) allows precise design creation by adding materials layer by layer through computer-controlled processes, offering unparalleled flexibility in designing and customizing architecture (Sangiorgio et al., 2022; Volpe et al., 2022; Souza et al., 2020).

Competitive performance and sustainability are required for these technologies to become established in the building market. Although there are numerous studies aimed at maximizing the performance of different 3D printing-based technologies there are few findings regarding a comparison of such technologies and their sustainability. In fact, various 3D printing technologies have been experimentally applied to the production of building components (Zhang et al., 2019). Among these, the principal or more promising methods based on material extrusion technologies include large-scale monolithic 3D printing in situ, prefabrication of 3D printed components, and the FDM-based formwork technique (Xiao et al., 2021; Burger et al., 2020) using large gantry cranes, small gantry cranes, and Fused Deposition Modelling (FDM) 3D printers, respectively. Moreover, several applications of 3D technology in the building industry focus on the use of concrete materials. Examples of applications include bridges, houses, offices and facilities (Mierzwiński et al., 2023).

Considering the current emphasis on environmental concerns, the environmental sustainability of concrete 3D printing technologies is imperative for their widespread adoption in industry. Consequently, numerous studies have been undertaken to evaluate the overall environmental impacts of these innovative solutions and ascertain whether they can serve as a more environmentally friendly alternative to traditional processes (Khan et al., 2021). The most commonly used methodology for quantifying and comparing the carbon footprint of both traditional casting and 3DCP is Life Cycle Assessment (LCA) (Balasbaneh and Ramli, 2020).

Concrete material production typically constitutes the most significant contributor to the overall environmental footprint of both traditional and 3D printed concrete structures, accounting for up to 97 % of the total impacts (Motalebi et al., 2023). Consequently, efforts have been made to enhance the sustainability of raw materials, although it remains an ongoing challenge (Bhattacherjee et al., 2021; Hottle et al., 2022; Salas et al., 2016). Indeed, AM offers promising advantages in terms of geometric complexity and the potential for optimizing infill, which can reduce material consumption and the environmental impact of concrete structures (Gislason et al., 2022).

The majority of literature on 3DCP focuses on the evaluation of concrete extrusion-based technologies (large-scale and prefabrication) and their comparison to traditional concrete casting and formwork prefabrication (Fernandez et al., 2023; Weng et al., 2020). For instance, Alhumayani et al. compared large-scale 3D printing with conventional construction demonstrating the sustainable potential of 3DCP (Alhumayani et al., 2020). Ebrahimi et al. (2022) emphasized the importance of raw materials material selection in thermal properties and sustainability of 3DCP. Liu et al. (2022) compared 3D printed structures to traditional precast concrete made with formwork, finding that 3D printed concrete becomes more sustainable relative to traditional methods as geometric complexity increases. Wu et al. assessed the use of a simple geometry 3D printed formwork for concrete casting processes, demonstrating the feasibility of the method and its improved sustainability (Wu et al., 2023).

Despite the recent interest and the increasing body of literature, several aspects related to the sustainability of 3D printing processes in the construction sector remain unexplored. There is a lack of systematic studies that assess various geometric configurations and infill patterns in 3D printed concrete structures. To the best of the authors' knowledge, no study has considered or highlighted the potential impact of geometric complexity and AM on the thermal properties and sustainability of concrete structures. Furthermore, traditional cast concrete scenarios have typically been compared to innovative 3D printing applications, but there is a scarcity of sustainability comparisons among different AM technologies. Moreover, there are recent 3D printing technologies (e.g., eggshell) that have yet to be investigated from an environmental sustainability perspective.

In this context, the present study focuses on assessing the environmental impacts and thermal properties of three distinct AM technologies and techniques that are undergoing significant development in the construction sector. These technologies include 3D printers based on large gantry cranes, small gantry cranes, and FDM, applied using the techniques of *monolithic construction*, *prefabrication*, and *FDM-based formwork* to cast concrete components. Specifically, the technologies and techniques are applied to design building envelope components consisting of a 3D printed cementitious mixture and thermal insulation based on cellulose fiber, with the configuration based on a sinusoidal geometry. Various configurations have been investigated, including variations in infill complexity and wall thickness, which were considered through thermal simulation analyses and LCA analysis.

This approach provides a comprehensive perspective on the sustainability of different AM technologies, elucidating their strengths and weaknesses. It also enhances our understanding of how geometric parameters within each technology can influence the overall environmental footprint of structures. Consequently, this study serves as a valuable decision-making tool for industrial applications and guides future research efforts.

The novelty of the proposed research is twofold: 1) for the first time, it has been investigated how different technologies and techniques can achieve a building envelope with thermal performance targets using a parametric modelling and analysis approach, and 2) an LCA analysis has been conducted to identify the advantages of various 3D printing technologies and techniques for building envelopes, providing valuable guidance for more sustainable future developments.

2. Materials and methods

This section outlines the methodological approach adopted in the current research work. Specifically, it begins by detailing the selected 3D printing technologies and related applications to achieve different configurations of the building envelope. Subsequently, the thermal performance analysis methodology to characterise the different walls is described. Finally, the LCA approach employed to assess the environmental impact of the technologies and related applications is elucidated. Fig. 1 summarises the proposed three-step methodological approach.

2.1. 3D printing technologies

In this section, various technologies and techniques of 3D printing for building envelopes are selected and discussed. The emphasis is placed on explaining the reasoning behind the choice of specific technologies and techniques. Finally, the different building envelope achievable are stated for each selected 3D printing approach.

The investigated techniques are selected based on the prevailing approaches in the literature (Xiao et al., 2021), which include: i) large-scale monolithic 3D printing in situ, ii) prefabrication of 3D printed components, iii) prefabricated 3D printing formwork, which, when produced with ultra-thin shells, is referred to as the "Eggshell" technique (Burger et al., 2020a,b). Consequently, the study focuses on these three aforementioned 3D printing techniques in the architecture, engineering, and construction (AEC) sector, briefly labelled as: i) *Monolithic*, ii) *Prefabrication*, and iii) *FDM-based formwork*. These distinct techniques leverage various 3D printing technologies. Among the available options, for the proposed work, the large gantry crane, small gantry crane 3D printing, and FDM 3D printers have been respectively
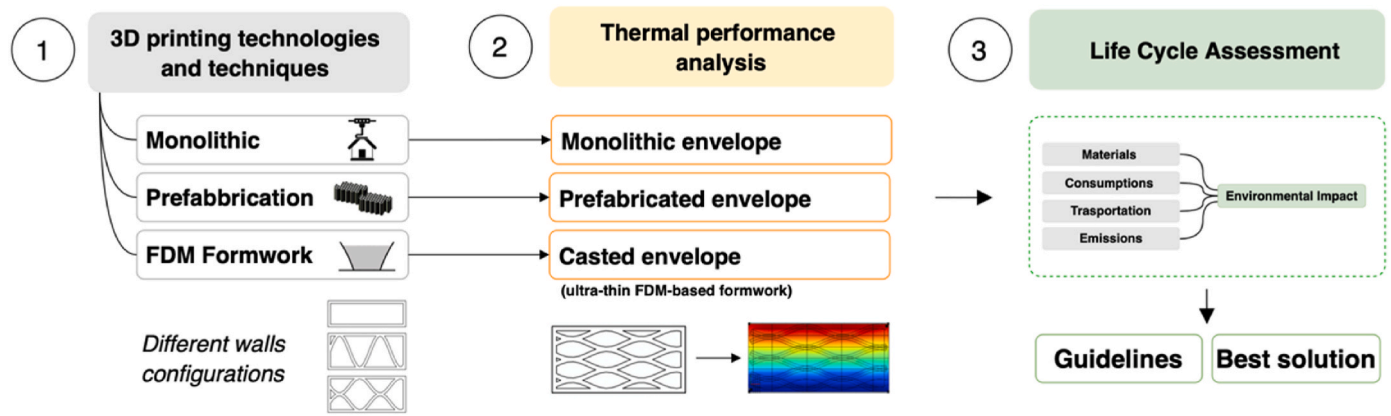
Fig. 1. The proposed three-step methodological approach.

chosen. Fig. 2 depicts the combination of technologies and techniques chosen for the analyses.

In the subsequent subsections, the rationale for the selection of specific technologies and usage techniques is justified in relation to market prevalence or potential capabilities. In addition, each technology and specific usage is described in detail. In the last one of these subsections, the potential building envelope configurations attainable with these techniques are presented.

2.1.1. Monolithic 3D printing with gantry system

The production process of monolithic construction takes place directly in situ. In this case, the building envelope is printed in situ as a single structure. This has the advantage of not needing to create and assemble multiple components. Every building storey is achieved in a single 3D printing session. Currently, there are three main technologies used to achieve large monolithic 3DCP: gantry system, cable-suspended solution and robotic arm (Parisi et al., 2023). Among these, the most widely used system (that has gained significant traction in the market) is the gantry system (Puzatova et al., 2022). The gantry system relies on a frame structure to provide support for the printer's extruder and its actuator, facilitating movements in various directions along the Cartesian coordinates X, Y, and Z (Labonnote et al., 2016). Notable companies

employing this system for achieving 3D printing of monolithic constructions include COBOD, Contour Crafting Corporation, and PERI Construction (Parisi et al., 2023).

In the proposed study, a COBOD 3D printing technology (model BOD2), specifically engineered for in situ concrete printing of large 3D structures, has been chosen for analysis (COBOD, 2023). This is a large machine with a print volume that can extend to approximately 15 m in width, 15 m in length, and 8 m in height. The printing speed can reach up to 1 m/s, and the layer thickness can go up to 300 mm. It requires a team of 3–4 people to operate. The materials used by the BOD2 are principally cementitious mixtures, which are blended with superplasticizers to attain the necessary fluidity for extrusion and a specific viscosity that prevents deformation after printing (Sangiorgio et al., 2022). The printer, for in situ production, requires support from additional machinery such as the Silo, Mini Batch, and a Concrete Piston Pump in immediate proximity to the construction site.

The Silo is used in the production of concrete as storage for dry cement which is used to produce 3D printable concrete. The Mini Batch is designed specifically to meet the needs of using a customized concrete mix, even utilizing locally available concrete if feasible for 3D printing. The device consists of an agitator pan mixer supported by three load cells, a two-compartment hopper for sand and aggregates, V-shaped feed
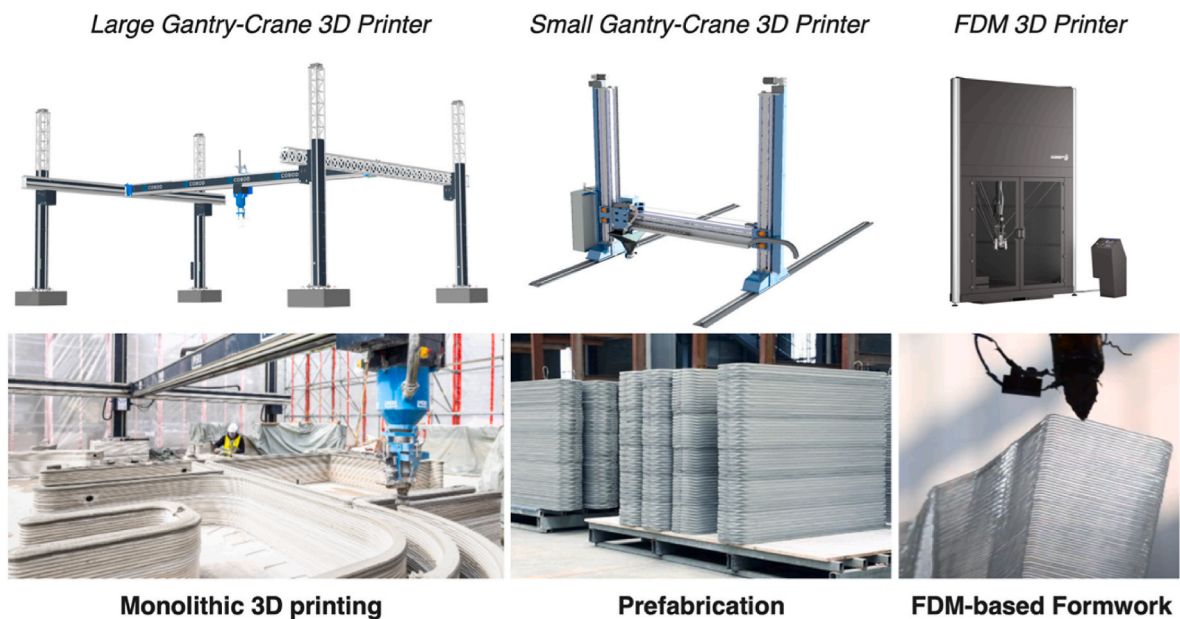

Fig. 2. Combination of technologies (3D printers in the upper part) and techniques (related applications in the lower part) chosen for the analyses. Image generated with the software Draw.io (2023) starting from figures of Gramaziokohler (2023), Peri (2023), Cobod (2023), Wasp (2023), Bemore3D (2023) and 3dadept (2023).

belts, a water tank, dosing equipment for two chemicals, and a control unit with a batching computer. The Concrete Piston Pump delivers the concrete material using a hydraulic piston pump with two cylinders. Specifically, the concrete pump receives the material from the COBOD Mini Batch Plant, which readies each material batch and then delivers it through the discharge gate to the pump's hopper.

2.1.2. 3D printing prefabrication with gantry system

The production process of 3D printing for prefabricated construction is adaptable for both in situ production and dedicated laboratories. By employing this technique, the building envelope is printed in distinct components that are subsequently assembled in situ (Volpe et al., 2021, 2023). The most commonly used machinery consists of gantry-crane-based 3D printers and robotic arms for 3D printing prefabrication. On the other hand, in prefabrication, the machines are medium or small-sized with printing volumes of about 3 m × 3 m x 3 m. In the market, there are various machines with similar performance and consumption that don't present significant differences in energy usage or printing speed (Puzatova et al., 2022). In the proposed research, the reference machinery is the "SMART 2500″ model, a granty-crane 3D printer from the company Be More 3D (Bemore3D SMART, 2023). Unlike large-scale printers, those designed for prefabrication can achieve thinner layer thicknesses, up to 60 mm, and speeds of up to 0.150 m/s. This allows for greater precision and the ability to achieve complex shapes. On the other hand, when the complexity of the geometry increases, it is necessary to reduce the printing speed, resulting in the disadvantage of longer printing times. Also, 3D printing for prefabrication requires support from additional machinery such as concrete mixers and concrete pumps. In this case, the dimensions of these additional machines are reduced since the amount of required cement is lower for each print compared to monolithic 3D printing applications.

2.1.3. The formwork with fused deposition modelling

The FDM-based formwork technique (Burger et al., 2020a,b) represents an innovative concrete structure fabrication process employing FDM 3D printing. It is centred on achieving thin formworks for concrete components, enabling greater geometric flexibility compared to conventional construction formworks. In accordance with Gebhard et al. (2020), the FDM-based formwork is a fabrication process where a thin mould is 3D printed, employing the on-demand processing strategy. Hence, the structure is produced by casting concrete within the 3D printed formwork. Several 3D printing technologies can be used to create formworks, but in the case of thin mould, FDM 3D printing emerges as a particularly suitable approach (Gebhard et al., 2022). The FDM-based formwork technique is still relatively uncommon on a global scale, but there are research works (Gebhard et al., 2022; Burger et al., 2023) and some companies demonstrating its potential (RepRep, 2023). Indeed, several industrial applications of this technique are currently being developed, proving its feasibility and possible advantages for building envelopes and components (FreeFAB; Aectual, 2023; Euronews, 2023).

The production process with the FDM-based formwork technique is adaptable for both in situ production and dedicated laboratories thanks to the utilization of small and easily transportable 3D printers. Furthermore, this approach offers an exceptionally high degree of design freedom, surpassing even that of prefabrication with gantry systems. Offering a wide scope of design freedom, it provides the chance to create building envelope assemblies with precise interlocking among different components. Consequently, it has been chosen among the technologies and applications worthy of investigation to explore its potential for achieving sustainable building envelopes.

In the proposed work, the chosen FDM machine is the Wasp WASP 3 MT HDP which has a printed volume of approximately 1 m × 1 m x 1 m (Wasp, 2023). This type of machine employs polylactic acid (PLA) pellets as the printing material. Thanks to recent research and technological advancements, PLA can now be sourced as recycled material

(Zero-Waste-Lab,). The printed layer diameter is extremely thin, reaching a maximum of 5 mm. Although, for the FDM-based formwork technique, a thickness of 1.5 mm suffices (Burger et al., 2020a,b). This facilitates the creation of exceptionally thin formworks, allowing for greater precision and intricate designs. On the other hand, one downside is the considerably extended production times.

2.1.4. The walls configurations

Once the combination of technologies and techniques has been chosen, different building envelope types (external walls) are specified for the subsequent analysis (thermal and LCA). For each technology, the goal is to achieve diverse configurations in order to comprehend how different technologies can improve the efficiency and sustainability of the building envelope. The selected internal infill has been defined a priori, incorporating a sinusoidal geometry, as it is widely recognized as the most common practice (Suntharalingam et al., 2021). Indeed, such geometry is effective both for lengthening the heat flow path between the internal and external shell of the wall and for avoiding collapses of the walls during the printing. In addition, the sinusoidal geometry is well suited to be refined or not depending on the printing resolution achievable by the production technology. The cavities formed by the sinusoidal geometry are to be filled with cellulose fiber-based insulation material.

In order to conduct analyses on different configurations, a parametric model of the component has been created using Rhino and Grasshopper software. By parameterizing the number of sinusoids (NS), wall thickness (T), wall length (X) and wall width (Y) this parametric model enables the attainment of all desired configurations. Fig. 3 displays the geometrical parameters.

In the following, the configurations for each technology are defined based on the limitations of the technology such as wall thickness and resolution (Sangiorgio et al., 2022).

  i) Monolithic 3D printing typically prints walls of considerable thicknesses, and they are constructed without pattern infill or with a simple one. As a consequence, the defined configurations to be printed with this technology include a wall thickness of 6 cm or 10 cm and a type without pattern infill or with a single internal sinusoid. To achieve the desired wall thickness, the nozzle size is selected accordingly (6 cm or 10 cm respectively). In turn, the layer height is selected to be compatible with the nozzle, with the choice being consistent with the limits declared in the COBOD technical specifications (Cobod, 2023). In particular, layer height is set at 3 cm when the nozzle is 6 cm and 4 cm when the nozzle is 10 cm. Monolithic printing by constructing elements directly in situ can realize elements of considerable length. Accordingly, the length of the corresponding configurations has been assumed to be 2.5 m.
 ii) Prefabricated concrete components can be printed with lower wall thicknesses. Consequently, a thickness of 4 cm or 6 cm has been defined. Also in this case, the nozzle size is selected
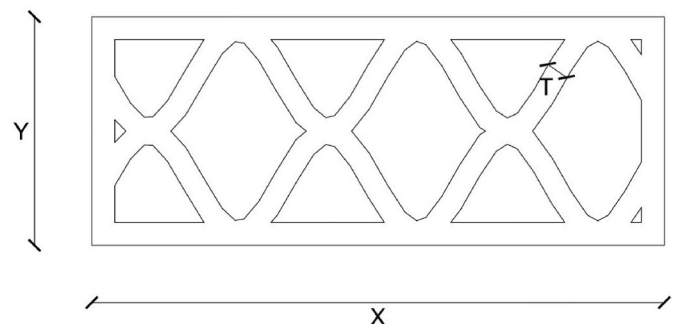

Fig. 3. Geometrical parameters: wall thickness (T), length (X) and width (Y).

accordingly (4 cm and 6 cm respectively). The layer height is set at 2 cm when the nozzle is 4 cm and 3 cm when the nozzle is 6 cm. Thanks to the greater precision of this technique and technology, the envelope can contain up to 4 internal sinusoids. The length of prefabricated elements must be consistent with the possibility of handling them, so it has been defined as 1 m.

iii) The FDM-based formwork technique is particularly versatile, as it involves printing an ultra-thin formwork, enabling wall thicknesses to vary from 6 cm to even more diminutive dimensions, such as 2 cm (used for the proposed formwork). The internal structure can encompass from 0 up to 6 sinusoids. In this case, a nozzle of 0.5 cm is used, consequently, the layer height is set at 0.25 cm. The length of the elements must take into account the common dimensions of the printers used for this type of technology (smaller than the previous ones). Consequently, a length of 0.6 m has been defined for the configurations associated with the FDM-based formwork production.

Fig. 4 shows a complete overview of the defined 3D printed envelope configuration classified according to the three types of printing technology. For each technology, as mentioned above, the length of the elements is kept constant while the wall thickness and number of sinusoids vary. Specifically, Fig. 4 displays all wall configurations defined for subsequent thermal and LCA analyses. Different element lengths have been considered consistent with the manufacturing technology. Therefore, elements of lengths of 250 cm, 100 cm and 60 cm were respectively considered for the monolithic, prefabrication and the FDM-based formwork technology production. In order to compare elements of different sizes, the LCA for the production of unit sizes of 1 square metre were subsequently considered.

2.2. Thermal analysis

The different configurations defined and their production technologies can be compared from the point of view of environmental impact under the same thermal performance. Thermal performance and the environmental impact of envelope production are related. Indeed, depending on the 3D printing technique used, it is possible to achieve target transmittance performance with different wall thicknesses and levels of geometric complexity. In turn, these thicknesses and complexities are linked to material quantity and printing times, influencing the LCA. In this study it has been opted to carry out an LCA analysis on envelope components with the same thermal transmittance. This analysis complies with the LCA ISO standard 14,040–44, which specifies that
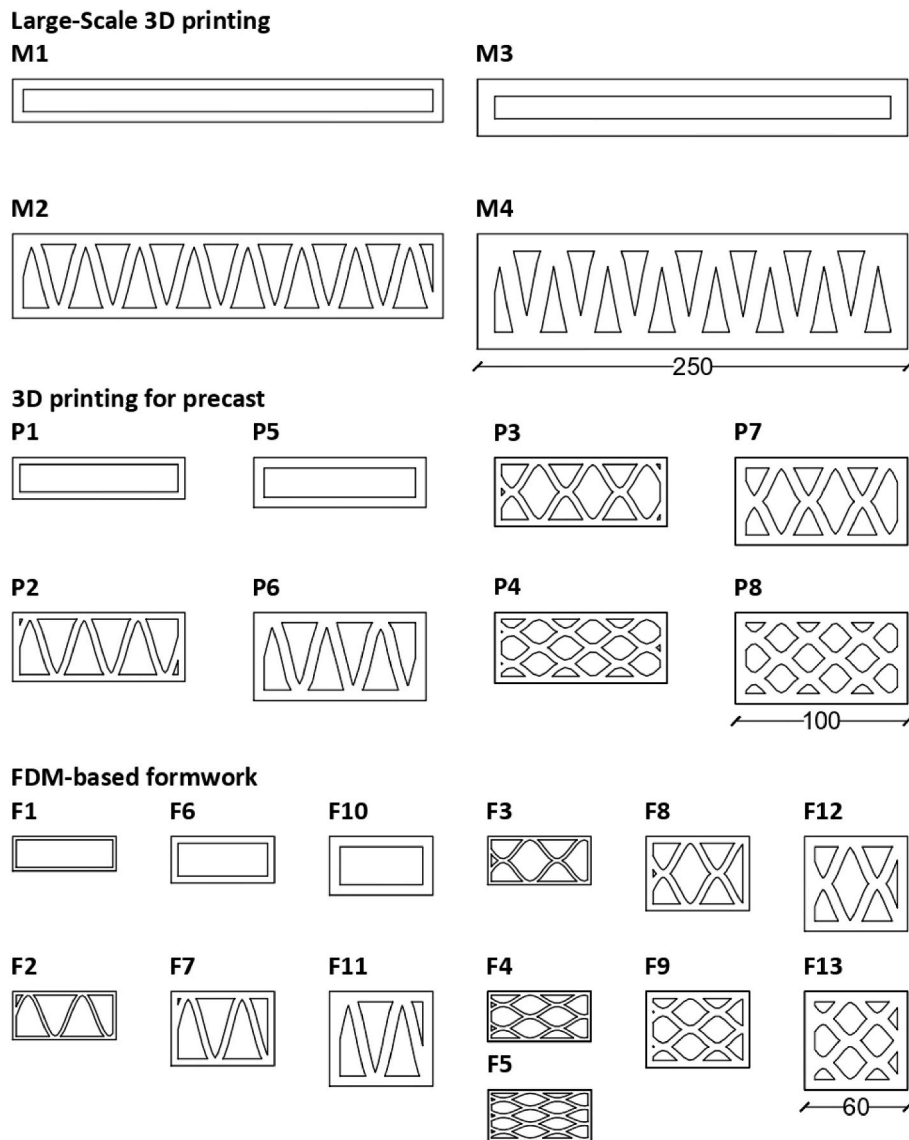

Fig. 4. The defined 3D printed envelope configurations.

it is essential to define structures with the same quantified performance to compare different scenarios. For this purpose, once the geometric parameters were defined, an iterative thermal analysis has been operated keeping the independent variables constant and varying the Y parameter in order to reach the same defined thermal transmittance value. The analysis was conducted using the Grassopper software. In particular, Grasshopper is a visual programming language that works as an extension of the 3D computer-aided design (CAD) application Rhinoceros. The analysis was conducted by developing an algorithm to create configurations based on the provided parameters. By adjusting these parameters, the geometry can vary accordingly. Additionally, another algorithm (connecting the THERM software and grasshopper) calculates the thermal transmittance of a given geometric section. This integration allows for an iterative modification of geometric parameters along with the evaluation of thermal transmittance. More in detail the software THERM uses two-dimensional (2D) conduction and radiation heat-transfer analysis based on the finite-element method, which can model the complicated geometries of building envelope. This method requires the division of the investigated model into a mesh made up of non-overlapping elements. This process is performed automatically by THERM using the Finite Quadtree method (THERM, 2023).

In particular, the thermal analysis has been performed according to the following three steps.

1. Geometry parametrization, as above described. Wall sinusoids number, wall thickness T and length X represent the independent variables as they have been defined for the different configurations, on the other hand, width Y constitutes the dependent variable as it is supposed to vary during the iterative thermal analysis until the thermal transmittance reaches the defined value.
2. Defining the thermal parameters. The constituent materials of the envelope components common to all configurations have been defined. Specifically, a cementitious mixture with a thermal conductivity of 0.28 W/(mK) has been chosen as the printing material. In addition, a cellulose fiber-based insulation material with a thermal conductivity of 0.04 W/(mK) has been defined as the cell-filling material. Finally, an overall target thermal transmittance common to all configurations has been established. The target thermal transmittance U value of 0.29 W/(m^{2}K) refers to Italian Ministerial Decree No. 162 of 26 June 2015 (DM, 2015) and particularly corresponds to climatic zone D.
3. Performing the iterative thermal analysis of each defined configuration. The thermal analysis has been carried out with the parametric model directly connected to a thermal analysis algorithm using Grasshopper based on THERM software. Once the geometry to be analyzed is connected, data on geometric areas, materials and relative thermal conductivity are entered into the program. The input data consist of the independent geometric parameters of the different defined configurations while the output data consists of the width Y obtained once the desired thermal transmittance value is achieved. Fig. 5 depicts a schematic representation of the iterative approach used to attain the target performance.
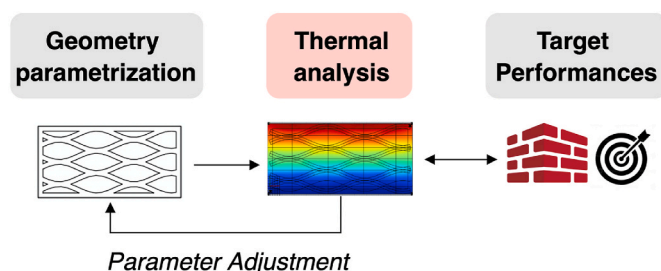

Fig. 5. The thermal analysis iterative procedure.

Table 1 resumes the different configurations investigated related to the printing technology and their parameters. In addition, the thermal transmittance value achieved by varying the geometric parameters is given for each configuration. Specifically, the transmittance is close to the target thermal transmittance value of 0.29 W/(m^{2}K) agreed for the case study. Each configuration has been subsequently analyzed with LCA to compare the environmental impact of printing technology at the same thermal performance conditions.

2.3. Life cycle assessment

The environmental impact analysis is performed according to the Life Cycle Assessment standardized methodology (Organization for standarization, 2004). This widely recognized framework consists of four iterative phases:

  i) Goal and scope definition;
 ii) Life Cycle Inventory (LCI);
iii) Life Cycle Impact Assessment (LCIA);
 iv) Results and discussion.

The LCA analysis was carried out using the dedicated software SimaPro 9.4. The analysis phases are detailed in the following subsections.

2.3.1. Goal, scope and scenarios definition

Given the growing interest and potential of 3D printing within the AEC sector, the present LCA analysis aims to evaluate the environmental impacts of different AM technologies and provide an in-depth comparison among them. Moreover, this study investigates the advantages and limitations of each technology, providing a better understanding of their effects on the environment and valuable insight for industries and researchers.

Three scenarios representing the aforementioned different 3D printing technologies and techniques were considered within the sustainability assessment:

- Monolithic 3D printing with a large gantry system (Scenario 1);
- Prefabrication of concrete 3D printing with a small gantry system (Scenario 2);
- Formwork with Fuse Deposition Modelling (Scenario 3).

All the wall configurations described in Section 2.1.4 and covered by the thermal analysis (Section 2.2) were investigated. Considering variable wall thickness and infill geometry to achieve the same thermal performance allows for the examination of the footprint of the scenarios based on the type and complexity of the structures, further highlighting potential advantages and challenges.

The functional unit is defined as the production of a section of an external wall of a single storey house with a standing area of 1 m^2 and an average thermal transmittance ranging between 0.28 W/m^2 K and 0.29 W/m^2 K. According to the literature, the unitary value of the standing area was chosen to guarantee the generality of the results and allow comparison with other analyses (Abdalla et al., 2021; Alhumayani et al., 2020). The transmittance value was chosen in accordance with the regulatory limit for buildings in Climate Zone D in Italy; this was adopted as a benchmark to ensure uniform thermal performance for the 3D printed walls across all scenarios. To meet this criterion, the 3D printed walls must vary in depth (and material use) depending on the scenario and the wall thickness and infill configuration. The necessary depth for each configuration is determined by the thermal analyses presented earlier. This enabled the attainment of configurations with equivalent quantified performance, specifically the thermal transmittance, serving as the reference unit for comparison among various scenarios. Given that the considered 3D printed envelopes are non-structural components of the building envelope (non-load-bearing),

Table 1
Configuration parameters and iterative thermal analysis results.

3D printing technology	Configuration number	Configuration Name	Wall thickness [cm]	Sinusoids number	X [cm]	Y [cm]	Thermal transmittance [W/m²K]
Large-Scale 3D printing	M1	Monolithic 6-0	6	0	250	25	0.2906
	M2	Monolithic 6-1	6	1	250	49	0.2919
	M3	Monolithic 10-0	10	0	250	33	0.2832
	M4	Monolithic 10-1	10	1	250	67	0.2915
3D printing for precast	P1	Prefabrication 4-0	4	0	100	24	0.2878
	P2	Prefabrication 4-1	4	1	100	40	0.2896
	P3	Prefabrication 4-2	4	2	100	40	0.2866
	P4	Prefabrication 4-4	4	4	100	41	0.2852
	P5	Prefabrication 6-0	6	0	100	29	0.2887
	P6	Prefabrication 6-1	6	1	100	51	0.2890
	P7	Prefabrication 6-2	6	2	100	51	0.2900
	P8	Prefabrication 6-4	6	4	100	53	0.2853
FDM-based formwork	F1	FDM Formwork 2-0	2	0	60	20	0.2941
	F2	FDM Formwork 2-1	2	1	60	28	0.2935
	F3	FDM Formwork 2-2	2	2	60	28	0.2890
	F4	FDM Formwork 2-4	2	4	60	29	0.2831
	F5	FDM Formwork 2-6	2	6	60	30	0.2866
	F6	FDM Formwork 4-0	4	0	60	27	0.2935
	F7	FDM Formwork 4-1	4	1	60	43	0.2896
	F8	FDM Formwork 4-2	4	2	60	43	0.2870
	F9	FDM Formwork 4-4	4	4	60	44	0.2849
	F10	FDM Formwork 6-0	6	0	60	34	0.2900
	F11	FDM Formwork 6-1	6	1	60	55	0.2918
	F12	FDM Formwork 6-2	6	2	60	55	0.2928
	F13	FDM Formwork 6-4	6	4	60	57	0.2868

the analysis did not consider the structural performance of different configurations.

2.3.2. System boundaries

The present LCA can be classified as "from cradle to gate" as it includes all phases from the extraction of raw materials to the wall construction phases. More specifically, it includes:

- Concrete raw materials extraction and transport; this phase takes into account the extraction, processing and transport of the raw materials required in the concrete mixture, including additives such as superplasticizer (i.e. polylactide) and reinforcement polypropylene (PP) fibers. Quantities and production processes of the different constituents are detailed in Section 2.3.3. The same concrete mixture was considered in all the 3D printing scenarios. By considering the transport phase, the direct transport of concrete constituents to the construction site was taken into account for the monolithic 3D printing case. In Scenarios 2 and 3, transport to the production facilities of the involved companies was considered as it was assumed that the precast and FDM-based formwork walls were produced in a site away from the construction one;
- PLA pellets production, pelletizing and transport for the FDM process were modelled (Scenario 3);
- Insulation material (cellulose fiber) production and transport (all scenarios);
- Materials mixing and pumping. This phase includes the electric energy consumption of the concrete mixing and pumping machines. Pumps with different powers were used in the three scenarios;
- 3D printing process for both concrete (Scenario 1 and 2) and PLA (Scenario 3). For the latter, in addition to electric energy consumption, compressed air use is also included (Wasp, 2023);
- Monolithic 3D printer, silos, concrete mixer and concrete pump transport to the building site for Scenario 1;
- Concrete wall transport from the company facilities to the building site for Scenarios 2 and 3;

- Prefabricated wall assembly in the construction site with the use of gantry cranes (Scenarios 2 and 3).

The machine production phases were excluded from the analysis (e. g. 3D printers, cranes, pumps). This is a common practice in LCA as the machines service life is typically much longer with respect to the considered system boundaries and their production would lead to negligible impacts (Bianchi et al., 2023).

The service life (Use phase) and end of life (EoL) of the walls was considered outside the system boundaries. It can be assumed that the impact of building service life is primarily related to ambient heating and cooling (Khalili Tari et al., 2023; Zabalza Bribián et al., 2009). Therefore, given that the functional unit (FU) was defined based on the thermal properties of the structures, the service life of the walls would not have a significant influence on the comparative analysis. Since the goal of the study is mainly focused on production processes, the EoL was not included in the analysis; in addition, at present there is not enough information to carry out a complete EoL modelling of the 3D printed structures, so it was considered out of the system boundaries.

Fig. 6 shows a schematic representation of the system boundaries and the phases included within the analysis.

2.3.3. Life Cycle Inventory

The Life Cycle Inventory (LCI) phase was performed using primary data measured by industrial partners during the 3D printing processes and secondary data obtained from literature research, mathematical formulae, and the Ecoinvent 3.1 database, included by default in SimaPro.

To model all the scenario configurations that vary in terms of wall thickness and infill, impacts per unit of different items (e.g. per kg of concrete produced or kWh used) were calculated in SimaPro and multiplied by the actual use of that resource for each production configuration. In this way, it was possible to quantify the impacts of several configurations by means of a spreadsheet.

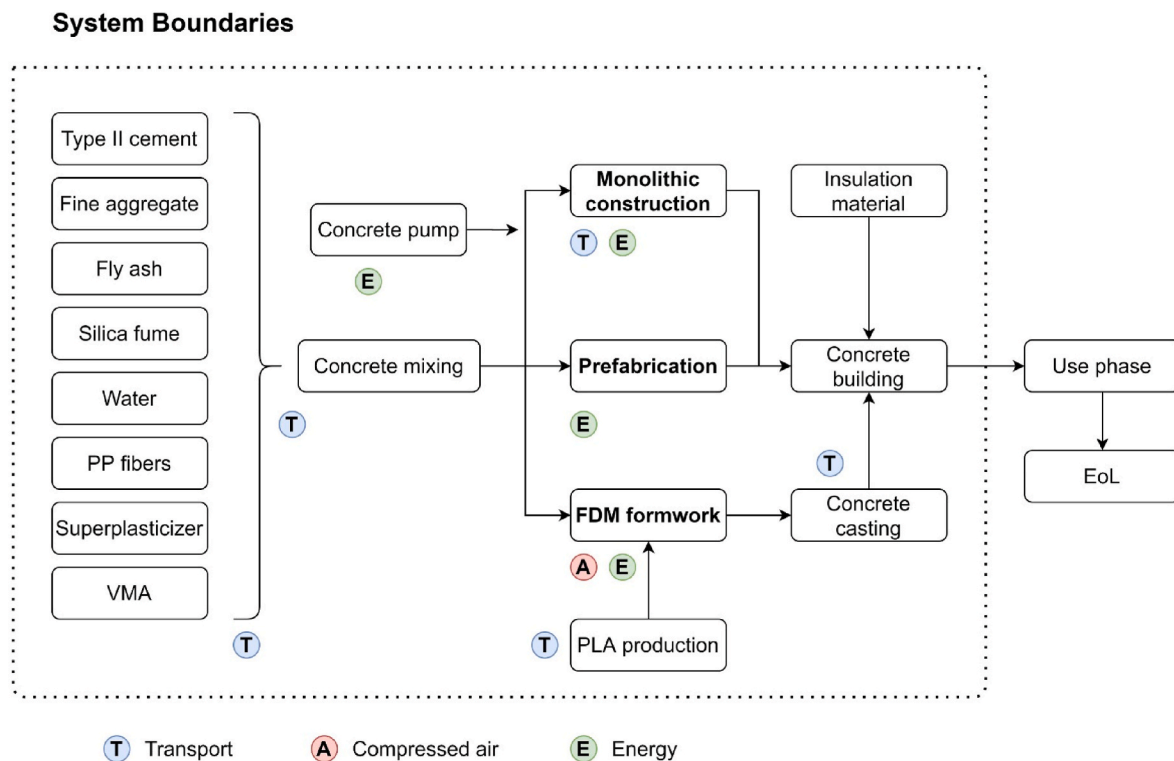Data concerning the percentage composition of the concrete mixture

System Boundaries

Fig. 6. System boundaries of the three considered scenarios.

were provided by an industrial partner operating in 3DCP. Raw materials were then modelled in SimaPro using datasets available in Ecoinvent. As well known in the literature (Hottle et al., 2022), concrete mix is mainly composed by:

- Cement and fly ash (modelled as Cement, alternative constituent 6–20 %);
- Micro silica fume (modelled as Silica sand);
- Fine aggregate (modelled as Sand);
- Water (modelled as Tap water).

In line with prior literature on 3DCP (Chen et al., 2021; Roux et al., 2023), the concrete utilized comprises approximately 25 % by weight of cement and fly ash, 10 % by weight of water, with the remaining portion primarily composed of micro silica fume and fine aggregate.

According to the commercial database, the models used for the selected materials also account for impacts associated with average transport distances to the building site. In addition to the standard components, small quantities of additives are introduced into the concrete mixture to adjust material viscosity, workability, and mechanical strength (Blazy and Blazy, 2021; Kubissa et al., 2022; Liu et al., 2021). Specifically, superplasticizer, Viscosity Modifying Admixture (VMA), and PP fibers were considered to be added in the concrete mixture. In accordance with previous literature studies, additives constitute less than 1.5 % of the total mixture weight, with each material accounting for about 0.5 % of the total weight (Hou et al., 2021; Ozbulut et al., 2020; Yin et al., 2015). Due to confidentiality reasons, the exact weight percentage of each constituent cannot be disclosed. The impacts of superplasticizer and VMA were obtained from the Ecoinvent database.

Among the available VMA materials, polylactide was selected (Ortiz-Álvarez et al., 2021). The production of PP fibers from PP granulates was modelled according to Yina et al. (2016), taking into account extrusion and hot stretching processes. According to this study, 1445

kW h of electric energy are required to produce 1 ton of PP fibers from raw PP, with waste accounting for 5 % of the initial material. This mixture results in a concrete density of approximately 2300 kg/m^3. The insulation material (cellulose fiber) was modelled in SimaPro using the Ecoinvent dataset.

The weights of concrete and insulation material for each configuration were computed based on the results of the thermal simulations. Utilizing the CAD model of the wall cross-section, which enables the determination of the specified thermal transmittance, it became feasible to determine the volume of concrete and cellulose fibers employed in each configuration. Consequently, factoring in the material densities, the weight of each material was determined. The overall material impacts were assessed by multiplying their weight by the unitary impact value quantified in SimaPro. The amount of concrete and insulation material used in each scenario configuration is reported in Appendix A.

As reported in the thermal analysis section, the different technologies lead to the production of concrete panels with different values of depth, length and height. Specifically, panels with length and height equal to 250 × 250 cm, 100 × 100 cm and 60 × 60 cm were considered for the monolithic, prefabrication and FDM-based formwork 3D printing techniques respectively. Hence, comparisons between the envelopes and the FU dimensions (1 × 1 m) were made to calculate the use of raw material in each scenario.

Similar to the assessment of concrete and insulation material weights, the weight of PLA pellets used in Scenario 3 (FDM-based formwork) was calculated based on the thermal simulation results. Starting from the CAD models of the wall, the formwork geometry was defined, taking into account a PLA wall thickness of 5 mm (equivalent to the nozzle diameter of the FDM printer used in this study). Consequently, the total material consumption for formwork production was determined by considering its volume and the density of PLA (1240 kg/m3) as reported by Barrasa et al. (2021). It's important to note that the formwork wall thickness, which matches the nozzle diameter of the FDM

3D printer, was kept consistent across all configurations in Scenario 3. Specifically, a 5 mm nozzle was chosen in accordance with the literature (Burger et al., 2023a,b).

For Scenario 3, different concrete wall thicknesses and shapes can be obtained just by changing the formwork geometry. This can be done using the same nozzle in the FDM process. On the other hand, in monolithic and prefabrication 3D printing, the wall thickness depends on the nozzle diameter; hence, in order to obtain different wall thicknesses, different nozzles must be used.

For each machine, a constant average printing speed was assumed, regardless of the nozzle diameter. This means that the printer's flow rate varies depending on the nozzle size, impacting the total printing time and electric energy consumption. Specifically, the unitary energy consumption (measured in kWh/kg of extruded material) decreases as the nozzle diameter increases. This enabled the quantification of the electric energy consumption of the machines per kilogram of extruded material. Therefore, considering the required amount of concrete or plastic in the selected configurations, the total energy demand was calculated. Similar considerations were applied to evaluate the energy consumption of concrete mixers and pumps, with the same mixing and pumping system being used for Scenarios 2 and 3. Data regarding the rated power and productivity of the machines were provided by the respective companies. Impacts associated with energy consumption, as modelled in the Ecoinvent database, were derived using the average Italian mix for low-voltage electric energy.

The FDM 3D printer requires 8 bars of compressed air for the vacuum-controlled build plate ('Large scale 3D printer | WASP 3 MT HDP,' n. d.). The calculation of the compressed air requirement took into account the necessary air flow rate (100 l/min) and the machine's productivity.

As far as the assembly phase for Scenarios 2 and 3 is concerned, the electric energy consumption of the tower crane was considered. A unitary energy requirement equal to 20 kW h/m^3 of concrete was taken from the literature (Pinky Devi and Palaniappan, 2014).

It was assumed that the construction company's site is located in Central Italy. Transport distances for raw materials to the company and the building site were assessed based on the geographical locations of suppliers and the routes recommended by Google Maps (Gradin and Åström, 2020). A transport distance of 500 km was adopted for all

Scenarios 2 and 3 concrete walls, encompassing potential building sites in most cities across Italy. A more detailed discussion of transport distances is provided in the sensitivity analysis (section 3.1).

Since in Scenario 1, the wall was built directly in situ, no additional concrete transport was required. The transport weights of the used machines (monolithic 3D printer, silos, concrete mixer, and pump) were provided by the involved company. The transport impacts of the machines were allocated to the functional unit by taking into account the standing area of the FU (1 m^2) and that of the entire building (a single-story house, approximately 80 m^2, $10 \times 8 \times 4 = 144$ m^2 of external wall standing area). Transport-related impacts were obtained from the Ecoinvent database, considering Euro 5 freight lorries. Table 2 reports LCI data related to the energy consumption of the machines and transport distances.

2.3.4. Life Cycle Impact Assessment

According to prior literature studies addressing the sustainability assessment of concrete structures, two impact categories were chosen to measure the potential environmental effects of the scenarios (Huang et al., 2019; Wong and Loo, 2022). In particular, the results of the Life Cycle Impact Assessment (LCIA) phase were expressed in terms of:

- Global Warming Potential (GWP), measured in kilograms of CO$_2$ equivalent (kg CO$_2$ eq) quantifies greenhouse gas emissions and their impact on climate change. The methodology of the International Panel on Climate Change (IPCC) was followed.
- Cumulative Energy Demand (CED), measured in megajoules (MJ) quantifies all direct and indirect energy usage from renewable and non-renewable sources throughout the phases included within the system boundaries. In addition, from a sustainability standpoint, 3D printing technologies exhibit different unitary impacts compared to traditional techniques, primarily due to machine energy consumption. Therefore, particular attention has been given to this environmental issue.

The dedicated LCA software SimaPro, with the Ecoinvent database, was employed to carry out the LCIA phase to translate the LCI data into possible environmental impacts.

Table 2
Relevant LCI data for machine use and transport for the three considered scenarios.

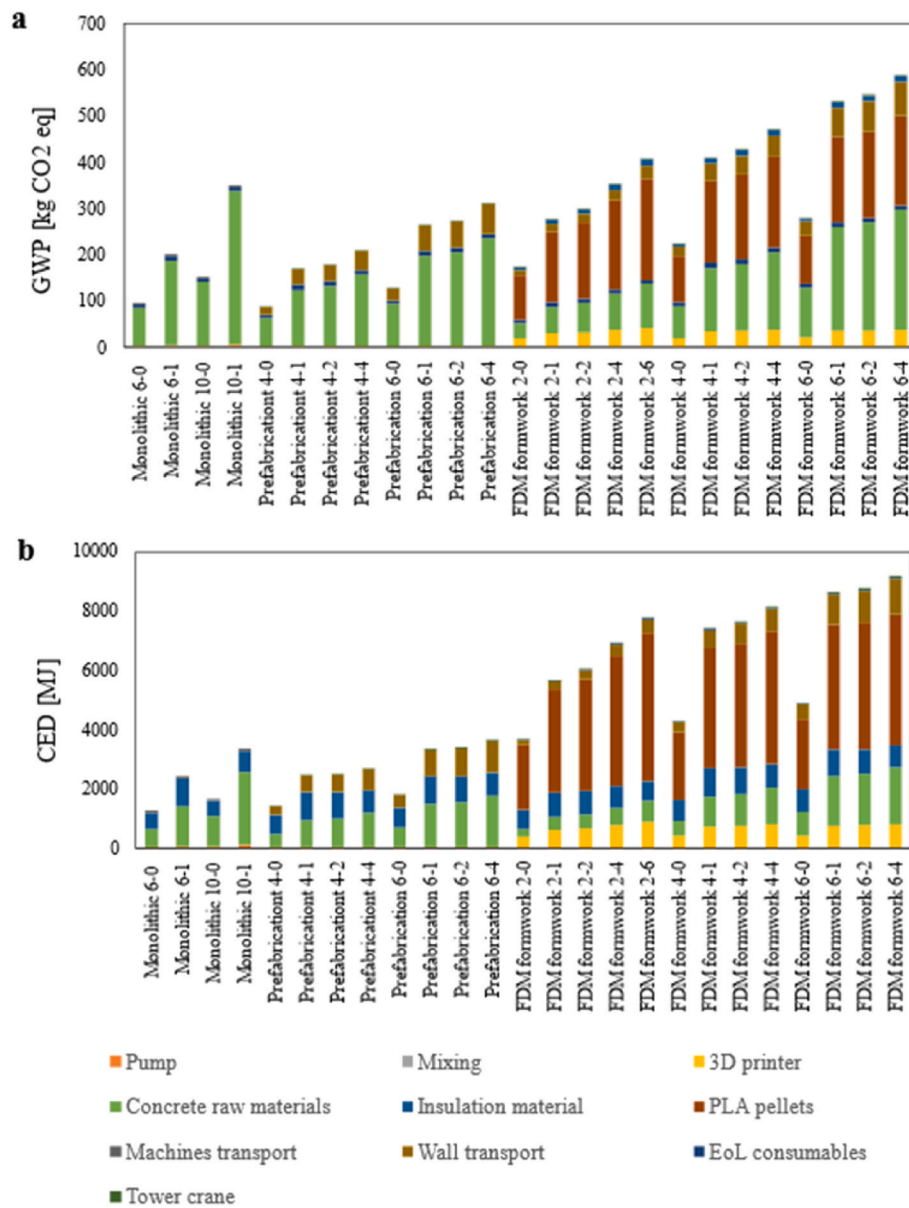|	Scenario 1	Scenario 2	Scenario 3
3D printer	Monolithic	Prefabrication	FDM formwork
Nozzle diameter [mm]	100 or 60 60	60 or 40 40	5
Absorbed power [kW]	1	5	1.5
Printing speed [mm/s]	100	85	40
Energy consumption [Wh/kg]	0.60 or 1.67 1.67	5.65 or 2.51 2.51	428.57
Compressed air [l/min]	/	/	100
Weight [kg]	5390	1000	250
Concrete mixer			
Absorbed power [kW]	7.5	2	2
Energy consumption [Wh/kg]	0.83	2.26	2.26
Weight [kg]	900	133	133
Pump			
Absorbed power [kW]	22	4	4
Energy consumption [Wh/kg]	13.22	4.52	4.52
Weight [kg]	1700	80	80
Tower crane			
Energy consumption [Wh/kg]	/	8.7	8.7
Transport, freight lorry			
Wall transport [km]	500		
PLA pellets [km]	180		

Fig. 7. LCIA results in terms of GWP (a) and CED (b) for all the considered configurations of the three scenarios.

3. Results and discussion

This section presents and discusses the results of the LCIA for both GWP and CED. Consequently, the impact of the three technologies and techniques (represented by the three scenarios) is analyzed. The results help to identify the advantages and disadvantages of the various techniques, along with valuable insights for improving the various processes from an environmental sustainability perspective.

Fig. 7 displays the results of the LCIA phase for all configurations in the three scenarios, presenting Global Warming Potential (Fig. 7a) and Cumulative Energy Demand (Fig. 7b).

It is noteworthy that both impact categories exhibit similar trends and percentage contributions. Appendix A also provides numerical results for LCIA and all data related to concrete, insulation material, and PLA weights for each scenario configuration. The envelope impacts are significantly influenced by the building technology used and the specific configuration, ranging from 88.26 kg CO_2 eq and 1257.72 MJ to 588.89 kg CO_2 eq and 9170.67 MJ.
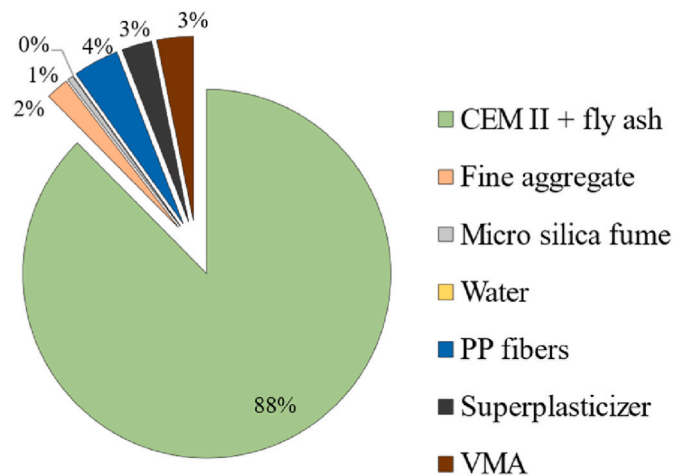

Fig. 8. Percentage contribution of the raw material impacts in terms of GWP used for concrete production.

3.1. The impact of large gantry system for monolithic construction

The impacts associated with monolithic 3D printing using a gantry system (Scenario 1) are primarily linked to concrete production, contributing as much as 95 % to the total impacts. This is attributed to the substantial amount of material utilized in constructing the envelope and the unitary impacts of concrete (approximately 660 kg CO_2 eq per m^3). This trend aligns with previous studies on both traditional and innovative 3D-printed concrete buildings (Khalili Tari et al., 2023; Liu et al., 2022).

The impacts of raw materials increase as the nozzle diameter and the number of sinusoids for the infill (i.e., the geometric complexity of the structure) increase. This is consistent with the simulation results, in which, as the nozzle diameter and the number of sinusoids increases, the wall depth required to achieve the defined thermal transmittance also increases. As a result, envelope weights and material impacts rise. Therefore, from an environmental perspective, thinner walls with simpler geometry represent a more sustainable solution.

Given the significance of raw materials in all the examined scenarios, the impacts of the concrete constituents were analyzed in detail in Fig. 8. As reported in the literature (Park et al., 2012), most of the impacts are associated with the production of type II Portland cement. The other traditional constituents, despite being present in large quantities, do not have significant impacts. Although the mass fraction of PP fibers is less than 1 %, it contributes to approximately 4 % of the total Global Warming Potential (GWP) value. This is primarily due to the polypropylene virgin material and, to a lesser extent, the energy consumption required. To enhance the sustainability of concrete mixes, sustainable alternatives to Portland cement can be employed, such as geopolymer concrete (Yao et al., 2020). Additionally, PP fibers made from recycled materials could be utilized, which would become more relevant if, in future developments, concrete mixes with higher reinforcement mass fractions are used for 3D printing applications (Demont et al., 2021).

The electric energy consumption related to the COBOD 2 3D printer and the mixing and pumping system is almost negligible, accounting for only about 1 % of the total impacts. In fact, the monolithic 3D printer has low energy consumption (1 kW) and high productivity, capable of extruding even more than 1500 kg of concrete per hour. These characteristics could encourage the widespread adoption of this technology on an industrial scale. The benefits of AM in terms of geometric complexity can be applied to the construction sector without a significant increase in energy usage. Hence, in line with previous literature, 3D printing technologies have the potential to reduce both the environmental and economic impacts of concrete constructions (Munir and Kärki, 2021; Weng et al., 2020).

The impacts of the insulation material (cellulose fibers) are considerably lower than those of concrete, typically ranging from 2 % to 7 % of the total GWP in Scenario 1. Cellulose fibers have a low density (50 kg/m3 (Brischke and Humar, 2017)) and low unitary GWP impacts (1.05 kg CO_2 eq). Therefore, even though the volume of insulation material used is comparable to that of concrete, it results in significantly lower impacts. On the other hand, regarding CED results, cellulose fibers account for up to 40 % of the total impacts. According to the Ecoinvent model, this is attributed to the energy required for their production (CED equal to 87.11 MJ per kg). However, since nuclear and renewable energy sources are primarily used, the associated CO_2 emissions remain low.

The impacts of machine transport (i.e., the monolithic printer, and the mixing and pumping machines) amount to 4.6 kg CO_2 eq and 75 MJ, contributing between 1 and 5 % of the total impact. Given the considerable distance of transport (500 km) and the substantial weight of the machines (almost 8000 kg in total), these values are relatively low. The reason is that the impacts of machine transport are distributed across the entire construction process, and overall, they are not considered critical. Furthermore, in situ construction eliminates the need to transport precast envelopes, offering environmental benefits. As the development and adoption of monolithic construction through 3D printing grow, it is expected that a greater number of companies will embrace this technology, leading to reduced average transport distances.

3.2. The impact of 3D printing prefabrication with gantry system

Similarly to Scenario 1, in Scenario 2 (prefabrication 3D printing), the impacts are primarily associated with the production and transportation of concrete raw materials, constituting 70–75 % of the total impacts. Indeed, the usage and impact of concrete are influenced by factors such as wall depth, geometric complexity, and printing nozzle diameter. Greater wall depth results in higher impact.

On the other hand, unlike the previous scenario, transportation plays a significant role in both GWP and CED in 3D printing prefabrication. In this case, freight lorries are necessary to transport the prefabricated envelopes to the construction site. In contrast, in Scenario 1 (monolithic construction), raw materials are shipped directly to the construction site, eliminating the need for additional transportation. The semi-finished products can weigh over 800 kg, and their transport is fully allocated to the functional unit, resulting in a contribution to impacts ranging from 5 % to 20 % of the GWP of Scenario 2. Therefore, in situ production for prefabrication technology could improve the sustainability of 3D printed buildings. In this additional scenario, the impacts related to machine transport will be lower than those in monolithic construction due to the reduced dimensions and weight of the required 3D printer (SMART 2500 printer). In that case, however, aspects such as time, labour and costs required to assemble and disassemble the machine should be considered for industrial applications also from an economic perspective.

The energy consumption associated with the SMART 2500 3D printer and the concrete preparation system is low and has minimal influence on the Life Cycle Impact Assessment (LCIA) results. Similarly, the tower crane required for the assembly phase results in negligible impacts.

If the same wall configuration is compared between Scenario 1 and Scenario 2 (e.g. monolithic 6–1 and Prefabrication 6–1, i.e. 6 cm of wall thickness and 1 internal Sinusoid), impacts of the prefabrication are higher than the monolithic construction. This is attributed to the additional transport phase required for the concrete envelopes. However, in the event of in situ production of the prefabricated components in Scenario 2, this disparity would be eliminated, resulting in comparable impacts. The advantage of 3D printing prefabrication lies in the ability to create more intricate shapes with thinner walls compared to the monolithic alternative. For example, the Prefabrication 4–0 configuration in Scenario 2 is more sustainable than any configuration in Scenario 1 due to its reduced wall depth and concrete usage. In addition, when printing in situ, the process is highly dependent on weather conditions, such as wind and rain. On the other hand, with prefabrication, it is feasible to conduct printing operations practically at any time.

3.3. The impact of FDM-based formwork for prefabrication techniques

Since FDM-based formwork construction is also a prefabrication technique, the same considerations regarding the transportation of components and machinery for in situ production apply in this case as well. However, in Scenario 3, the main contributor to the total CED and GWP values 3 is represented by PLA pellet production (33–60 % of the total, depending on the configuration and impact category), leading to total impacts generally higher than those of Scenarios 1 and 2.
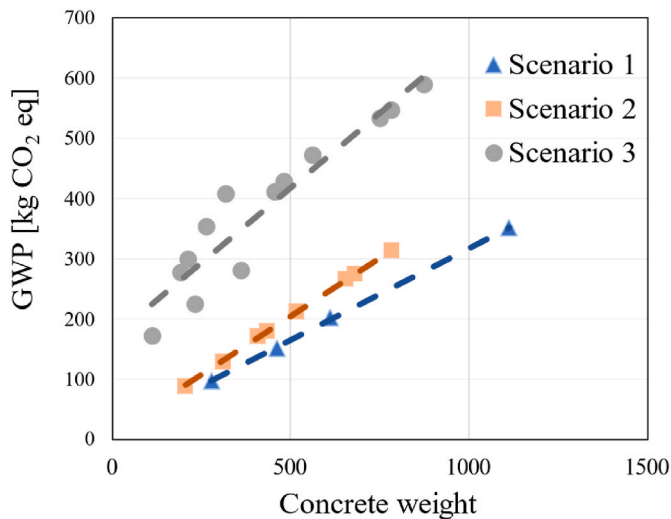
Fig. 9. GWP of the three scenarios as a function of concrete weight for every structure configuration.

PLA is well-known for its sustainability and biodegradability as a thermoplastic material (Bałdowska-Witos et al., 2020), with emissions of 3.05 kg CO_2 eq per kg of virgin material. This is significantly lower than other synthetic alternatives currently utilized for FDM processes, such as ABS (4.54 kg CO_2 eq/kg) and polyamide (8.24 kg CO_2 eq). However, the production of 3D printed formworks requires a substantial amount of material (31.4–63.1 kg). Specifically, the quantity of PLA increases with the number of sinusoids in the infill pattern, while it is less dependent on the concrete wall thickness (Appendix A). Regardless of the final concrete layer thickness, the FDM printing nozzle and PLA wall thickness remain constant at 5 mm. In general, a more complex infill pattern results in increased usage of both PLA and concrete, which reduces the overall sustainability of the produced part. Consequently, FDM-based formwork configurations with high wall thickness and complex infills are the alternatives that exhibit the highest impacts among those considered in this study.

On the other hand, FDM-based formwork technique has the potential to produce extremely thin concrete walls, which would be challenging to achieve using other methods. This approach has the potential to reduce the consumption of raw materials. In fact, configurations like FDM formwork 2–0 and 2–1 exhibit the lowest concrete usage (and impacts) among all available options. Plastic FDM printers, however, have significantly lower productivity compared to concrete extrusion machines, with a maximum output of only 3.5 kg/h. This lower productivity is primarily due to the much smaller nozzle dimensions (0.5 cm). Consequently, the FDM printer requires much more energy per kilogram of extruded material and contributes to 6–10 % of the total impacts in the given scenario. For the future advancement of this technology, enhancements in the FDM process and material utilization could

potentially make Scenario 3 the most sustainable alternative. Envelope transport and assembly exhibited impacts similar to those observed in Scenario 2.

3.4. The importance of saving concrete

From the conducted analysis, it becomes evident from an environmental standpoint the importance of reducing cement usage at the expense of printing and production speed. To emphasize this aspect, Fig. 9 illustrates the LCIA results in terms of GWP as a function of concrete weight.

More specifically, Fig. 9 displays the LCIA results in terms of GWP relative to concrete weight. Across all scenarios, a heavier configuration corresponds to higher environmental impacts, displaying an almost linear relationship between total GWP and concrete weight. Among configurations with the same concrete weight, Scenario 1 emerges as the most sustainable alternative. When compared to Scenario 2, it exhibits lower impacts because the building is 3D printed in situ and doesn't require envelope transport. This gap can be eliminated by directly implementing prefabrication technology at the construction site. Scenario 3 incurs higher impacts due to transport and the use of the FDM printer. Future improvements in FDM-based technology are expected, driven by the adoption of more renewable energy sources and recycled polymers.

It's also worth noting that Scenario 1 results in the heaviest buildings due to the wider nozzle diameter. In contrast, Scenarios 2 and 3 offer weight reduction due to thinner walls, leading to sustainability improvements.

3.5. Sensitivity analysis

In order to further investigate the analyses and assess how the results can change with varying inputs, a sensitivity analysis was conducted. Specifically, for this analysis, Scenario 3 was chosen, and in particular, the most critical configuration of FDM formwork 4–2. As mentioned earlier, this technology is the most recent and has the potential for significant improvement in the years ahead. The total GWP was calculated by varying relevant input data one at a time. The impact range of different items in terms of kg of CO_2 eq was assessed by considering alternatives characterized by varying degrees of sustainability (Table 3).

Table 3
Variation range of input data and item impacts used in the sensitivity analysis.

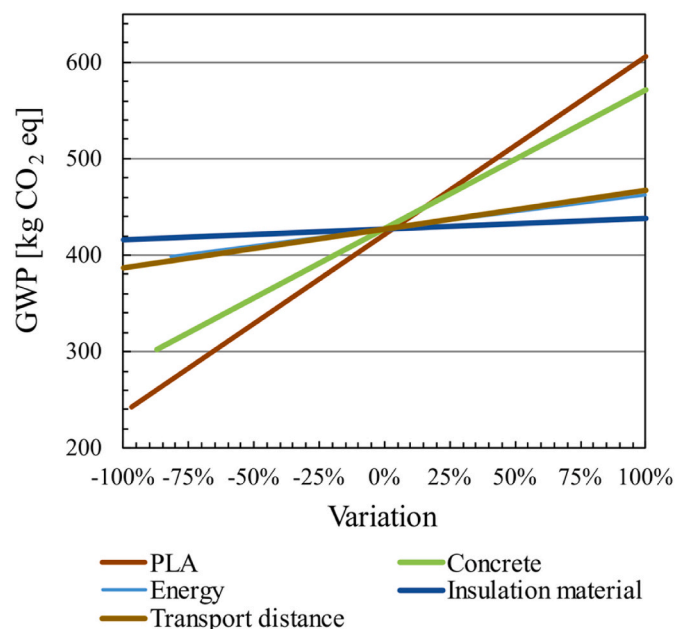|	Variation range		Unit	Data source
	Min	Max		
PLA	0.112	6.16	kg CO_2 eq/kg	Min: recycled PLA production (Maga et al., 2019)
Insulation material	0	2.1	kg CO_2 eq/kg	Max: foam glass (Ecoinvent)
Electric energy	0.0199	0.212	kg CO_2 eq/kWh	Min: photovoltaic source for electric energy (Ecoinvent)
Concrete	89	1320	kg CO_2 eq/ton	Min: sustainable geopolymer concrete (Yao et al., 2020)
Wall transport	0	1000	km	Min: printing on construction site

Fig. 10. Sensitivity analysis for Scenario 3 FDM formwork 4–2 configuration.

Literature research and Ecoinvent 3.1 were utilized to define possible alternatives and to establish the range of impacts. For example, foam glass was selected as a possible alternative to cellulose fibers as it is a widely used insulation material in the construction sector and it is characterized by higher unitary impacts with respect to the baseline material (Rodrigues et al., 2023). A maximum variation range of ±100 % was defined (Bianchi et al., 2022).

Fig. 10 illustrates the results of the sensitivity analysis. The impact values (y-axis) were obtained as a function of the input data percentage variation (x-axis). Among all factors, the impacts of concrete and PLA have the most significant influence on the overall environmental impacts. The utilization of sustainable concrete (with impacts up to 85 % lower than traditional mixtures) could potentially decrease the total environmental impacts of Scenario 3 by approximately 27 %. Regarding the other scenarios, this impact reduction could be even greater than in Scenario 3 due to the contributions of raw materials to the overall carbon footprint. This improvement can be applied to traditional cast concrete buildings as well. Moreover, the use of recycled PLA (or blends of recycled and virgin polymers) and the printed formwork recycling could offer substantial sustainability benefits. In fact, the impacts of recycled PLA are nearly negligible compared to the baseline scenario and can reduce the impacts of the walls by 43 %. This would bring the impacts of Scenario 3 close to those of Scenarios 1 and 2, even with the same envelope configurations. This improvement is currently under investigation and a recent study proved that the used formwork can be recycled after concrete casting (Burger et al., 2023b).

Regardless of the scenario under consideration, additional impact reduction can be achieved by using more sustainable energy sources and minimizing transport distances. Specifically, for the analyzed configuration, the use of renewable energy and the reduction of transport distances can reduce the total scenario footprint by 7 % and 9 %, respectively.

A potential enhancement for these scenarios is represented by the use of robotic arms instead of traditional 3D printers. The focus on this topic is significant due to the growing interest in the use of robots for 3D printing in the construction sector. Owing to their high efficiency, robots can exhibit low energy absorption, making them a sustainable alternative to traditional systems (Mohammad et al., 2020). Additionally, in the case of FDM formwork printing, they can eliminate the need for compressed air usage during printing. From a sustainability perspective, the results showed that the 3D printer's energy consumptions are not the most relevant contributors. Therefore, even if the robotic system were capable of reducing printing energy absorption by 50 %, the overall reduction in impacts in Scenario 2 (prefabrication) would be at most 2.5 %, depending on the configuration. Thus, the results of this study would have been very similar if robotic arms were considered as moving systems for the investigated scenarios. A slightly higher reduction would be obtained for the FDM-printed formwork since, in that scenario, the printer's energy consumption is more impactful.

4. Conclusions

The introduction of 3D printing technology into the construction sector represents not merely an evolution but a revolution in construction methods. It offers unprecedented possibilities, redefines design, enhances performance, and fosters sustainability in building and architecture. In this context, for the first time, the proposed research investigates the thermal properties and environmental impacts of three emerging AM technologies to achieve building envelopes. In particular, 3D printing based on large gantry cranes, small gantry cranes, and FDM technologies are investigated in the application of monolithic construction (scenario 1), prefabrication (scenario 2), and FDM-based formwork techniques (scenario 3), respectively.

For the first time, an investigation has been conducted on how these

three approaches can be used to achieve different configurations of building envelopes with specific target performances. An LCA has been conducted to delve into the potential sustainable use of these technologies and techniques. As a result, this comprehensive study yielded the following valuable insights into the sustainability and performance of the above mentioned technologies and techniques.

- In all the scenarios, concrete production represents one of the most impactful phases, accounting for up to 95 % of the total environmental impacts.
- In general, as the number of sinusoids in the infill and wall thickness increase, an increment in material use and impacts is observed. Hence, thin walls produced using prefabrication and FDM-based formwork techniques could enhance envelopes' sustainability by reducing raw concrete impacts while maintaining the same thermal performance.
- The use of 3D printers for monolithic constructions and prefabrication has low energy consumption and high productivity. Hence, the utilization of energy and resources to maintain operative the 3D printing process is low (about 1 % of the total footprint). In addition, such printers appear to be the most sustainable options if the same geometrical configurations are compared.
- Formwork production in FDM-based formwork technique strongly increases the scenario impacts due to raw PLA production and machine energy consumption. On the other hand, this technology is relatively new, and sensitivity analysis indicates significant improvement potential. Indeed, FDM-based formwork technique impacts could be reduced using recycled material and sustainable electric energy sources; this would make Scenario 3 impacts close to the other two.

These findings provide valuable insights for both researchers and construction companies utilizing 3DCP to enhance the sustainability of their construction processes.

Future work will focus on different infill configurations and possible improvements. Life Cycle Costing analyses will be carried out to provide a comprehensive view of the economic impacts of the scenarios. These results, along with the LCA study, will provide a complete decision-making tool for the use of 3D printing technologies in the construction sector.

CRediT authorship contribution statement

Iacopo Bianchi: Writing – original draft, Visualization, Validation, Software, Methodology, Investigation, Formal analysis, Data curation, Conceptualization. **Stelladriana Volpe:** Writing – original draft, Visualization, Validation, Software, Methodology, Investigation, Formal analysis, Data curation, Conceptualization. **Francesco Fiorito:** Writing – review & editing, Validation, Supervision, Software, Resources, Conceptualization. **Archimede Forcellese:** Writing – review & editing, Validation, Supervision, Software, Resources, Conceptualization. **Valentino Sangiorgio:** Writing – review & editing, Writing – original draft, Visualization, Validation, Supervision, Software, Resources, Methodology, Investigation, Formal analysis, Data curation, Conceptualization.

Declaration of competing interest

The authors declare that they have no known competing financial interests or personal relationships that could have appeared to influence the work reported in this paper.

Data availability

Data will be made available on request.

Appendinx A.

Scenario	Weight [kg]				Global Warming Potential [kg CO$_2$ eq]										
	Total	Concrete	Insulation	PLA	Total	Pump	Mixing	3D printer	Tower crane	Concrete	Insulation	PLA	Machines transport	Wall transport	EoL
Monolithic 6-0	283.92	277.73	6.19		95.47	1.06	0.09	0.18		83.06	6.50		4.58	0.00	0.00
Monolithic 6-1	620.45	609.81	10.64		201.04	2.33	0.19	0.39		182.37	11.18		4.58	0.00	0.00
Monolithic 10-0	468.86	462.88	5.98		151.31	1.77	0.15	0.11		138.43	6.28		4.58	0.00	0.00
Monolithic 10-1	1119.37	1111.13	8.25		350.39	4.24	0.35	0.25		332.29	8.66		4.58	0.00	0.00
Prefabricationt 4-0	211.52	204.16	7.36		87.06	0.23	0.06	0.44	0.68	61.06	7.73			16.87	0.00
Prefabricationt 4-1	416.92	406.16	10.77		169.13	0.45	0.13	0.88	1.35	121.46	11.31			33.55	0.00
Prefabricationt 4-2	441.79	431.60	10.19		178.41	0.48	0.14	0.93	1.43	129.07	10.70			35.65	0.00
Prefabricationt 4-4	526.02	517.28	8.74		210.18	0.57	0.16	1.12	1.72	154.70	9.18			42.73	0.00
Prefabrication 6-0	316.36	308.88	7.48		127.51	0.34	0.10	0.30	1.03	92.37	7.86			25.52	0.00
Prefabrication 6-1	664.59	653.95	10.64		264.50	0.72	0.21	0.63	2.17	195.57	11.17			54.02	0.00
Prefabrication 6-2	688.11	678.02	10.09		273.24	0.75	0.21	0.65	2.25	202.77	10.60			56.01	0.00
Prefabrication 6-4	790.85	782.13	8.72		312.14	0.86	0.25	0.75	2.60	233.90	9.16			64.61	0.00
FDM formwork 2-0	118.93	111.47	7.47	31.41	171.57	0.12	0.00	17.74	0.37	33.34	7.84	96.75		9.21	6.20
FDM formwork 2-1	201.66	192.03	9.64	49.85	275.79	0.21	0.00	28.16	0.64	57.43	10.12	153.53		15.86	9.83
FDM formwork 2-2	221.65	212.48	9.17	53.81	298.40	0.23	0.00	30.39	0.71	63.54	9.63	165.72		17.55	10.62
FDM formwork 2-4	273.63	265.16	8.47	62.93	353.03	0.29	0.00	35.54	0.88	79.30	8.90	193.80		21.90	12.41
FDM formwork 2-6	326.84	319.09	7.75	71.62	406.50	0.35	0.00	40.45	1.06	95.43	8.14	220.58		26.36	14.13
FDM formwork 4-0	239.97	231.73	8.23	32.65	223.57	0.26	0.00	18.44	0.77	69.30	8.65	100.57		19.14	6.44
FDM formwork 4-1	468.21	457.10	11.11	57.79	410.17	0.50	0.00	32.64	1.52	136.70	11.67	177.97		37.76	11.40
FDM formwork 4-2	493.39	482.87	10.53	59.84	427.39	0.53	0.00	33.80	1.60	144.41	11.06	184.30		39.89	11.81
FDM formwork 4-4	571.05	561.81	9.23	63.84	471.86	0.62	0.00	36.06	1.87	168.02	9.70	196.60		46.41	12.59
FDM formwork 6-0	369.60	360.80	8.80	33.89	278.76	0.40	0.00	19.14	1.20	107.90	9.24	104.38		29.81	6.69
FDM formwork 6-1	761.28	750.85	10.44	60.24	532.30	0.83	0.00	34.03	2.49	224.55	10.96	185.54		62.03	11.88
FDM formwork 6-2	790.27	780.51	9.76	61.09	546.29	0.86	0.00	34.50	2.59	233.42	10.25	188.13		64.48	12.05
FDM formwork 6-4	882.05	873.40	8.65	63.14	588.89	0.96	0.00	35.66	2.90	261.20	9.09	194.47		72.15	12.46

References

3dadept. https://3dadept.com/yihe-would-be-able-to-build-donald-trump-s-wall-using-3d-printing/, 2023. November 2023.

Abdalla, H., Parvez Fattah, K., Abdallah, M., Tamimi, A.K., Tajani, F., Locurcio, M., Di Liddo, F., 2021. Environmental footprint and economics of a full-scale 3D-printed house, 2021 Sustainability 13, 11978. https://doi.org/10.3390/SU132111978, 11978 13.

Aectual | 3D printed architecture & interiors [WWW Document]. November 2023 https://www.aectual.com/.

Alhumayani, H., Gomaa, M., Soebarto, V., Jabi, W., 2020. Environmental assessment of large-scale 3D printing in construction: a comparative study between cob and concrete. J. Clean. Prod. 270, 122463 https://doi.org/10.1016/J.JCLEPRO.2020.122463.

Balasbaneh, A.T., Ramli, M.Z., 2020. A comparative life cycle assessment (LCA) of concrete and steel-prefabricated prefinished volumetric construction structures in Malaysia. Environ. Sci. Pollut. Control Ser. 27, 43186–43201. https://doi.org/10.1007/S11356-020-10141-3/FIGURES/9.

Bałdowska-Witos, P., Kruszelnicka, W., Kasner, R., Tomporowski, A., Flizikowski, J., Kłos, Z., Piotrowska, K., Markowska, K., 2020. Application of LCA method for assessment of environmental impacts of a polylactide (PLA) bottle shaping, 2020 Polymers 12, 388. https://doi.org/10.3390/POLYM12020388. Page 388 12.

Barrasa, J.O., Ferrández-Montero, A., Ferrari, B., Pastor, J.Y., 2021. Characterisation and modelling of PLA filaments and evolution with time. Polymers 13. https://doi.org/10.3390/POLYM13172899.

Bemore3D. https://bemore3d.com/, 2023. July 2023.

Bemore3D SMART. https://bemore3d.com/productos/, 2023. November 2023.

Bhattacherjee, S., Basavaraj, A.S., Rahul, A.V., Santhanam, M., Gettu, R., Panda, B., Schlangen, E., Chen, Y., Copuroglu, O., Ma, G., Wang, L., Basit Beigh, M., Mechtcherine, V., 2021. Sustainable materials for 3D concrete printing. Cem. Concr. Compos. 122, 104156 https://doi.org/10.1016/J.CEMCONCOMP.2021.104156.

Bianchi, I., Forcellese, A., Simoncini, M., Vita, A., Castorani, V., Arganese, M., De Luca, C., 2022. Life cycle impact assessment of safety shoes toe caps realized with reclaimed composite materials. J. Clean. Prod. 347, 131321 https://doi.org/10.1016/J.JCLEPRO.2022.131321.

Bianchi, I., Forcellese, A., Simoncini, M., Vita, A., 2023. Mechanical characterization and sustainability assessment of recycled EVA for footwears, 2023 Int. J. Adv. Des. Manuf. Technol. 1–12. https://doi.org/10.1007/S00170-023-11332-1.

Blazy, J., Blazy, R., 2021. Polypropylene fiber reinforced concrete and its application in creating architectural forms of public spaces. Case Stud. Constr. Mater. 14, e00549 https://doi.org/10.1016/J.CSCM.2021.E00549.

Brischke, C., Humar, M., 2017. Performance of the bio-based materials. Perform. Bio-based Build. Mater. 249–333. https://doi.org/10.1016/B978-0-08-100982-6.00005-7.

Burger, J., Lloret-Fritschi, E., Scotto, F., Demoulin, T., Gebhard, L., Mata-Falcón, J., Gramazio, F., Kohler, M., Flatt, R.J., 2020a. Eggshell: ultra-thin three-dimensional printed formwork for concrete structures. 3D Print. Addit. Manuf. 7 (2), 48–59. https://doi.org/10.1089/3dp.2019.0197.

Burger, J., Lloret-Fritschi, E., Taha, N., Scotto, F., Demoulin, T., Mata-Falcón, J., Gramazio, F., Kohler, M., Flatt, R.J., 2020b. Design and fabrication of a non-standard, structural concrete column using eggshell: ultra-thin, 3D printed formwork. In: Second RILEM International Conference on Concrete and Digital Fabrication: Digital Concrete 2020, 2. Springer International Publishing, pp. 1104–1115. https://doi.org/10.1007/978-3-030-49916-7_105.

Burger, J., Aejmelaeus-Lindström, P., Gürel, S., Niketić, F., Lloret-Fritschi, E., Flatt, R.J., Gramazio, F., Kohler, M., 2023a. Eggshell Pavilion: a reinforced concrete structure fabricated using robotically 3D printed formwork. Constr. Robot. 1–21 https://doi.org/10.1007/s41693-023-00090-x.

Burger, J., Lloret-Fritschi, E., Akermann, M., Schwendemann, D., Gramazio, F., Kohler, M., 2023b. Circular formwork: recycling of 3D printed thermoplastic formwork for concrete. Technol. Archit. Des. 7, 204–215. https://doi.org/10.1080/24751448.2023.2245724.

Chen, Y., Zhang, Y., Pang, B., Liu, Z., Liu, G., 2021. Extrusion-based 3D printing concrete with coarse aggregate: printability and direction-dependent mechanical performance. Construct. Build. Mater. 296, 123624 https://doi.org/10.1016/J.CONBUILDMAT.2021.123624.

Cobod, 2023. https://cobod.com/. July 2023.

Demont, L., Ducoulombier, N., Mesnil, R., Caron, J.F., 2021. Flow-based pultrusion of continuous fibers for cement-based composite material and additive manufacturing: rheological and technological requirements. Compos. Struct. 262, 113564 https://doi.org/10.1016/J.COMPSTRUCT.2021.113564.

DM, 2015. Decreto Ministeriale 26 Giugno 2015. Applicazione Delle Metodologie di Calcolo Delle Prestazioni Energetiche e Definizione Delle Prescrizioni e dei Requisiti Minimi Degli Edifici, Governo Italiano. Italy, 2015. Ministero dello Sviluppo Economico, Roma. https://www.mimit.gov.it/index.php/it/normativa/decreti-interministeriali/decreto-interministeriale-26-giugno-2015-applicazione-delle-metodologie-di-calcolo-delle-prestazioni-energetiche-e-definizione-delle-prescrizioni-e-dei-requisiti-minimi-degli-edifici. November 2023.

Draw.io. https://draw.io, 2023. November 2023.

Ebrahimi, M., Mohseni, M., Aslani, A., Zahedi, R., 2022. Investigation of thermal performance and life-cycle assessment of a 3D printed building. Energy Build. 272, 112341 https://doi.org/10.1016/J.ENBUILD.2022.112341.

Euronews, 2023. https://www.euronews.com/my-europe/2019/02/28/sustainable-architecture-thanks-to-3d-printers. November 2023.

Fernandez, L.I.C., Caldas, L.R., Mendoza Reales, O.A., 2023. Environmental evaluation of 3D printed concrete walls considering the life cycle perspective in the context of

social housing. J. Build. Eng. 74, 106915 https://doi.org/10.1016/J.JOBE.2023.106915.

FreeFAB. https://www.freefab.com/. November 2023.

Gebhard, L., Mata-Falcón, J., Anton, A., Burger, J., Lloret-Fritschi, E., Reiter, L., Dillenburger, B., Gramazio, F., Kohler, M., Flatt, R., Kaufmann, W., 2020. Aligned interlayer fibre reinforcement and post-tensioning as a reinforcement strategy for digital fabrication. In: Second RILEM International Conference on Concrete and Digital Fabrication: Digital Concrete 2020, vol. 2. Springer International Publishing, pp. 622–631. https://doi.org/10.1007/978-3-030-49916-7_63.

Gebhard, L., Burger, J., Mata-Falcón, J., Lloret Fritschi, E., Gramazio, F., Kohler, M., Kaufmann, W., 2022. Towards efficient concrete structures with ultra-thin 3D printed formwork: exploring reinforcement strategies and optimisation. Virtual Phys. Prototyp. 17 (3), 599–616. https://doi.org/10.1080/17452759.2022.2041873.

Gislason, S., Bruhn, S., Breseghello, L., Sen, B., Liu, G., Naboni, R., 2022. Porous 3D printed concrete beams show an environmental promise: a cradle-to-grave comparative life cycle assessment. Clean Technol. Environ. Policy 24, 2639–2654. https://doi.org/10.1007/S10098-022-02343-9/FIGURES/12.

Gradin, K.T., Åström, A.H., 2020. Comparative life cycle assessment of car disc brake systems—case study results and method discussion about comparative LCAs. Int. J. Life Cycle Assess. 25, 350–362. https://doi.org/10.1007/s11367-019-01704-9.

Gramaziokohler. https://gramaziokohler.arch.ethz.ch/web/d/forschung/330.html, 2023. November 2023.

Grandviewresearch. https://www.grandviewresearch.com/, 2023. July 2023.

Hossain, M.A., Zhumabekova, A., Paul, S.C., Kim, J.R., 2020. A review of 3D printing in construction and its impact on the labour market". Sustainability 12, 8492. https://doi.org/10.3390/su12208492.

Hottle, T., Hawkins, T.R., Chiquelin, C., Lange, B., Young, B., Sun, P., Elgowainy, A., Wang, M., 2022. Environmental life-cycle assessment of concrete produced in the United States. J. Clean. Prod. 363, 131834 https://doi.org/10.1016/J.JCLEPRO.2022.131834.

Hou, S., Duan, Z., Xiao, J., Ye, J., 2021. A review of 3D printed concrete: performance requirements, testing measurements and mix design. Construct. Build. Mater. 273, 121745 https://doi.org/10.1016/J.CONBUILDMAT.2020.121745.

Huang, H., Wang, T., Kolosz, B., Andresen, J., Garcia, S., Fang, M., Maroto-Valer, M.M., 2019. Life-cycle assessment of emerging CO2 mineral carbonation-cured concrete blocks: comparative analysis of CO2 reduction potential and optimization of environmental impacts. J. Clean. Prod. 241, 118359 https://doi.org/10.1016/J.JCLEPRO.2019.118359.

Khalili Tari, M., Reza Faraji, A., Aslani, A., Zahedi, R., 2023. Energy simulation and life cycle assessment of a 3D printable building. Clean. Mater. 7, 100168 https://doi.org/10.1016/J.CLEMA.2023.100168.

Khan, M.S., Sanchez, F., Zhou, H., 2020. 3-D printing of concrete: beyond horizons. Cement Concr. Res. 133, 106070 https://doi.org/10.1016/j.cemconres.2020.106070.

Khan, S.A., Koç, M., Al-Ghamdi, S.G., 2021. Sustainability assessment, potentials and challenges of 3D printed concrete structures: a systematic review for built environmental applications. J. Clean. Prod. 303, 127027 https://doi.org/10.1016/J.JCLEPRO.2021.127027.

Kubissa, W., Wilińska, I., Jaskulski, R., 2022. Study on the effect of VMA admixture for concrete cured under different conditions on air permeability and sorptivity. Construct. Build. Mater. 346, 128350 https://doi.org/10.1016/J.CONBUILDMAT.2022.128350.

Labonnote, N., Rønnquist, A., Manum, B., Rüther, P., 2016. Additive construction: State-of-the-art, challenges and opportunities. Autom. Constr. 72, 347–366. https://doi.org/10.1016/J.AUTCON.2016.08.026.

Liu, X., Lai, G., Guan, J., Qian, S., Wang, Z., Cui, S., Gao, F., Jiao, Y., Tao, R., 2021. Technical optimization and life cycle assessment of environment-friendly superplasticizer for concrete engineering. Chemosphere 281, 130955. https://doi.org/10.1016/J.CHEMOSPHERE.2021.130955.

Liu, S., Lu, B., Li, H., Pan, Z., Jiang, J., Qian, S., 2022. A comparative study on environmental performance of 3D printing and conventional casting of concrete products with industrial wastes. Chemosphere 298, 134310. https://doi.org/10.1016/J.CHEMOSPHERE.2022.134310.

Maga, D., Hiebel, M., Thonemann, N., 2019. Life cycle assessment of recycling options for polylactic acid. Resour. Conserv. Recycl. 149, 86–96. https://doi.org/10.1016/J.RESCONREC.2019.05.018.

Marketsandmarkets. https://www.marketsandmarkets.com/. July 2023.

Mierzwiński, D., Łach, M., Gądek, S., Lin, W., Tran, D., Korniejenko, K., 2023. A brief overview of the use of additive manufacturing of con-create materials in construction. Acta Innov. 48, 22–37. https://doi.org/10.32933/ActaInnovations.48.2.

Mohammad, M., Masad, E., Al-Ghamdi, S.G., 2020. 3D concrete printing sustainability: a comparative life cycle assessment of four construction method scenarios, 2020 Buildings 10, 245. https://doi.org/10.3390/BUILDINGS10120245. Page 245 10.

Motalebi, A., Khondoker, M.A.H., Kabir, G., 2023. A systematic review of life cycle assessments of 3D concrete printing. Sustain. Oper. Comput. https://doi.org/10.1016/J.SUSOC.2023.08.003.

Munir, Q., Kärki, T., 2021. Cost analysis of various factors for geopolymer 3D printing of construction products in factories and on construction sites. Recycling 6 (3), 60. https://doi.org/10.3390/RECYCLING6030060.

Organization for standarization, I., 2004. Environmental management - life cycle assessment - principles and framework (ISO 14040:2006). Environ. Manag. Syst. Requir. 44.

Ortiz-Álvarez, N., Lizarazo-Marriaga, J., Brandão, P.F.B., Santos-Panqueva, Y., Carrillo, J., 2021. Rheological properties of cement-based materials using a

biopolymer viscosity modifying admixture (BVMA) under different dispersion conditions. Cem. Concr. Compos. 124, 104224 https://doi.org/10.1016/J. CEMCONCOMP.2021.104224.

Ozbulut, O.E., Jiang, Z., Harris, D.K., Jiang, Z., Fang, Y., Guo, Y., Amat, C., Ismail, K.N., Ibrahim, M., Azmi, N.J., 2020. Influence of superplasticizer on performance of cement – bottom ash concrete. IOP Conf. Ser. Earth Environ. Sci. 476 (1), 012025 https://doi.org/10.1088/1755-1315/476/1/012025.

Parisi, F., Sangiorgio, V., Parisi, N., Mangini, A.M., Fanti, M.P., Adam, J.M., 2023. A new concept for large additive manufacturing in construction: tower crane-based 3D printing controlled by deep reinforcement learning. Construct. Innovat. https://doi.org/10.1108/CI-10-2022-0278.

Park, J., Tae, S., Kim, T., 2012. Life cycle CO2 assessment of concrete by compressive strength on construction site in Korea. Renew. Sustain. Energy Rev. 16, 2940–2946. https://doi.org/10.1016/J.RSER.2012.02.014.

Peri. https://www.peri.com/en, 2023. November 2023.

Pinky Devi, L., Palaniappan, S., 2014. A case study on life cycle energy use of residential building in Southern India. Energy Build. 80, 247–259. https://doi.org/10.1016/J. ENBUILD.2014.05.034.

Puzatova, A., Shakor, P., Laghi, V., Dmitrieva, M., 2022. Large-scale 3D printing for construction application by means of robotic arm and Gantry 3D Printer: a Review. Buildings 12 (11), 2023. https://doi.org/10.3390/buildings12112023.

RepRep. https://bigrep.com/ebooks/fast-custom-concrete/, 2023. November 2023.

Rodrigues, C., König, J., Freire, F., 2023. Prospective life cycle assessment of a novel building system with improved foam glass incorporating high recycled content. Sustain. Prod. Consum. 36, 161–170. https://doi.org/10.1016/J.SPC.2023.01.002.

Roux, C., Kuzmenko, K., Roussel, N., Mesnil, R., Feraille, A., 2023. Life cycle assessment of a concrete 3D printing process. Int. J. Life Cycle Assess. 28, 1–15. https://doi.org/10.1007/s11367-022-02111-3.

Salas, D.A., Ramirez, A.D., Rodríguez, C.R., Petroche, D.M., Boero, A.J., Duque-Rivera, J., 2016. Environmental impacts, life cycle assessment and potential improvement measures for cement production: a literature review. J. Clean. Prod. 113, 114–122. https://doi.org/10.1016/J.JCLEPRO.2015.11.078.

Sangiorgio, V., Parisi, F., Fieni, F., Parisi, N., 2022. The new boundaries of 3D-printed clay bricks Design: printability of complex internal geometries. Sustainability 14 (2), 598. https://doi.org/10.3390/su14020598.

Sati, A.S.E., Mantha, B.R.K., Dabous, S.A., de Soto, B.G., 2021. Classification of Robotic 3D Printers in the AEC Industry. ISARC, Proceedings of the International Symposium on Automation and Robotics in Construction. United Arab Emirates, IAARC, Dubai, pp. 924–931. https://doi.org/10.22260/ISARC2021/0002.

Souza, M.T., Ferreira, I.M., de Moraes, E.G., Senff, L., de Oliveira, A.P.N., 2020. 3D printed concrete for large-scale buildings: an overview of rheology, printing parameters, chemical admixtures, reinforcements, and economic and environmental prospects. J. Build. Eng. 32, 101833 https://doi.org/10.1016/j.jobe.2020.101833.

Suntharalingam, T., Upasiri, I., Gatheeshgar, P., Poologanathan, K., Nagaratnam, B., Santos, P., Rajanayagam, H., 2021. Energy performance of 3d-printed concrete walls: a numerical study. Buildings 11 (10), 432. https://doi.org/10.3390/buildings11100432.

Therm. https://windows.lbl.gov/therm-software-downloads, 2023. November 2023.

Volpe, S., Sangiorgio, V., Petrella, A., Coppola, A., Notarnicola, M., Fiorito, F., 2021. Building envelope prefabricated with 3D printing technology. Sustainability 13 (16), 8923. https://doi.org/10.3390/su13168923.

Volpe, S., Sangiorgio, V., Fiorito, F., Varum, H., 2022. Overview of 3D construction printing and future perspectives: a review of technology, companies and research progression. Architect. Sci. Rev. https://doi.org/10.1080/00038628.2022.2154740.

Volpe, S., Sangiorgio, V., Petrella, A., Notarnicola, M., Varum, H., Fiorito, F., 2023. 3D printed concrete blocks made with sustainable recycled material. VITRUVIO-Int. J. Architect. Technol. Sustain. 8, 70–83. https://doi.org/10.4995/vitruvio-ijats.2023.18832.

Wasp, 2023. Large scale 3D printer | WASP 3MT HDP [WWW Document], n.d. URL. https://www.3dwasp.com/en/wasp-3mt-hdp-big-3d-printer/. August 2023.

Weng, Y., Li, M., Ruan, S., Wong, T.N., Tan, M.J., Ow Yeong, K.L., Qian, S., 2020. Comparative economic, environmental and productivity assessment of a concrete bathroom unit fabricated through 3D printing and a precast approach. J. Clean. Prod. 261, 121245 https://doi.org/10.1016/J.JCLEPRO.2020.121245.

Wong, R.W.M., Loo, B.P.Y., 2022. Sustainability implications of using precast concrete in construction: an in-depth project-level analysis spanning two decades. J. Clean. Prod. 378, 134486 https://doi.org/10.1016/J.JCLEPRO.2022.134486.

Wu, X., He, J., Tian, J., Tan, X., Hu, S., Zheng, Y., Wang, W.-W., Zhang, W., 2023. Shear behaviors of engineered cementitious composites to seawater sea-sand concrete (ECC-to-SSSC) interfaces cast using 3D-printed pre-grooving formwork: mechanical properties, characterization, and life-cycle assessment. J. Build. Eng. 78, 107636 https://doi.org/10.1016/J.JOBE.2023.107636.

Xiao, J., Ji, G., Zhang, Y., Ma, G., Mechtcherine, V., Pan, J., Wang, L., Ding, T., Duan, Z., Du, S., 2021. Large-scale 3D printing concrete technology: current status and future opportunities. Cement Concr. Compos. 122, 104115 https://doi.org/10.1016/j.cemconcomp.2021.104115.

Yao, Y., Hu, M., Di Maio, F., Cucurachi, S., 2020. Life cycle assessment of 3D printing geo-polymer concrete: an ex-ante study. J. Ind. Ecol. 24, 116–127. https://doi.org/10.1111/JIEC.12930.

Yin, S., Tuladhar, R., Shi, F., Combe, M., Collister, T., Sivakugan, N., 2015. Use of macro plastic fibres in concrete: a review. Construct. Build. Mater. 93, 180–188. https://doi.org/10.1016/J.CONBUILDMAT.2015.05.105.

Yina, S., Tuladhar, R., Sheehan, M., Combe, M., Collister, T., 2016. A life cycle assessment of recycled polypropylene fibre in concrete footpaths. J. Clean. Prod. 112, 2231–2242. https://doi.org/10.1016/J.JCLEPRO.2015.09.073.

Zabalza Bribián, I., Aranda Usón, A., Scarpellini, S., 2009. Life cycle assessment in buildings: state-of-the-art and simplified LCA methodology as a complement for building certification. Build. Environ. 44, 2510–2520. https://doi.org/10.1016/J.BUILDENV.2009.05.001.

Zero-waste-lab. https://thenewraw.org/Zero-Waste-Lab. July 2023.

Zhang, J., Wang, J., Dong, S., Yu, X., Han, B., 2019. A review of the current progress and application of 3D printed concrete. Compos Part A Appl Sci Manuf 125, 105533. https://doi.org/10.1016/J.COMPOSITESA.2019.105533.